

NASA/ASEE SUMMER FACULTY RESEARCH FELLOWSHIP PROGRAM

MARSHALL SPACE FLIGHT CENTER

THE UNIVERSITY OF ALABAMA

FUEL OPTIMAL MANEUVERS OF SPACECRAFT

ABOUT A CIRCULAR ORBIT

Prepared By:	Thomas E. Carter, Ph.D.
Academic Rank:	Associate Professor
University and Department:	Eastern Connecticut State College Mathematical Sciences
NASA/MSFC:	
Division:	Control Systems Division
Branch:	Dynamics & Trajectory Analysis Branch
MSFC Counterpart:	Harry J. Buchanan
Date:	August 20, 1982
Contract No.	NGT 01-002-099 The University of Alabama

FUEL OPTIMAL MANEUVERS OF SPACECRAFT

ABOUT A CIRCULAR ORBIT

By

Thomas E. Carter

Associate Professor of Mathematical Sciences

Eastern Connecticut State College

Willimantic, Connecticut

ABSTRACT

Fuel optimal maneuvers of spacecraft relative to a body in circular orbit are investigated using a point mass model in which the magnitude of the thrust vector is bounded. All nonsingular optimal maneuvers consist of intervals of full thrust and coast and are found to contain at most seven such intervals in one period. Only four boundary conditions where singular solutions occur are possible. Computer simulation of optimal flight path shapes and switching functions are found for various boundary conditions. Emphasis is placed on the problem of soft rendezvous with a body in circular orbit.

## ACKNOWLEDGEMENTS

The author expresses appreciation to Stan Carroll of the Dynamics and Trajectory Analysis Branch of the George C. Marshall Space Flight Center whose suggestions and insights were of much value to this project. He also thanks Roger Burroughs of the Flight Mechanics Branch of the George C. Marshall Space Flight Center who wrote the computer program which was used to solve the two-point-boundary value problems and who instructed the author in the use of this program.

## LIST OF FIGURES

<u>Figure No.</u>	<u>Title</u>	<u>Page</u>
1	Nature of Fuel Optimal Thrusting Sequence in Deep Space . . . . .	IX-8
2	Nature of Fuel Optimal Thrusting Sequence about a Point Moving in Circular Orbit . . . . .	IX-8
3	A Seven Phase Optimal Thrusting Sequence in One Period. . . . .	IX-10
4	The Absolute Value of $q$ Over One Period for the Seven Phase Optimal Thrusting Sequence .	IX-10
5	Switching Function and Flight Path for $X(0) = (0, 0)$ , $V(0) = (1, 0)$ , $X(TF) =$ $(0, 1)$ , $V(TF) = (0, 0)$ . . . . .	IX-15
6	Switching Function and Flight Path for $X(0) = (0, 0)$ , $V(0) = (0, 0)$ , $X(TF) =$ $(1, 1)$ , $V(TF) = (0, 0)$ . . . . .	IX-15
7	Switching Function and Flight Path for $X(0) = (0, 0)$ , $V(0) = (1, 0)$ , $X(TF) =$ $(0, 1)$ , $V(TF) = (-1, 0)$ . . . . .	IX-15
8	Switching Function and Flight Path for $X(0) = (0, 0)$ , $V(0) = (1, 0)$ , $X(TF) =$ $(0, 1)$ , $V(TF) = (1, 0)$ . . . . .	IX-16
9	Switching Function and Flight Path for $X(0) = (0, 0)$ , $V(0) = (1, 0)$ , $X(TF) =$ $(0, 0)$ , $V(TF) = (0, 1)$ . . . . .	IX-16
10	Switching Function and Flight Path for $X(0) = (0, 0)$ , $V(0) = (1, 0)$ , $X(TF) =$ $(0, 1)$ , $V(TF) = (0, 1)$ . . . . .	IX-16
11	Comparison of Switching Functions and Flight Paths for Deep Space and 435 KM. Altitude Circular Orbit: $X(0) = (1000,$ $1000)$ , $V(0) = (0, 0)$ , $X(TF) =$ $(0, 0)$ , $V(TF) = (0, 0)$ . . . . .	IX-17

LIST OF FIGURES (CONTINUED)

<u>Figure No.</u>	<u>Title</u>	<u>Page</u>
12	Comparison of Switching Functions and Flight Paths for Deep Space and 435 KM. Altitude Circular Orbit: $X(0) = (0, 1000)$ , $V(0) = (10, 0)$ , $X(TF) = (0, 0)$ , $V(TF) = (0, 0)$ . . . . .	IX-18
13	Switching Function and Flight Path for Different Flight Times for 435 KM. Circular Orbit: $X(0) = (1000, 0)$ , $V(0) = (0, 0)$ , $X(TF) = (0, 0)$ , $V(TF) = (0, 0)$ . . . . .	IX-19
14	Insertion of Mass From Elliptical into 435 KM. Circular Orbit: $X(0) = (0, 1000)$ , $V(0) = (0, 0)$ , $X(TF) = (0, 0)$ , $V(TF) = (0, 0)$ , Optimal Maneuver Requires Mid-Course Thrust . . . . .	IX-20
15	An Optimal Maneuver with Four Thrusts and Three Coasts in One Period (5600 SEC): $X(0) = (0, 0)$ , $V(0) = (0, 0)$ $X(TF) = (-73000, 0)$ , $V(TF) = (0, 35)$ . . .	IX-20

## CONTENTS

### FUEL OPTIMAL MANEUVERS OF SPACECRAFT ABOUT A CIRCULAR ORBIT

- I. Introduction
- II. Mathematical Analysis
  - 1. Solutions in the Orbital Plane
  - 2. Solutions Out of the Orbital Plane
- III. Computer Simulations
- IV. Conclusions

## I. INTRODUCTION

Most of the immediate applications of space involve a body in circular orbit. Fuel optimal maneuvers of a spacecraft relative to such a body constitute the subject of this investigation.

We assume the spacecraft to be a point mass with a variable thrust vector of bounded magnitude. The mass of the spacecraft is assumed constant over a fixed flight time  $t_f$  and a minimum fuel maneuver will be regarded as a maneuver in which the integral of the magnitude of the thrust is minimized. The position  $x$  and velocity  $v$  of the spacecraft are relative to a coordinate system fixed in the rotating body whose angular speed is  $\Omega$ . The positive  $x_1$  axis is in the direction of the orbital velocity, the positive  $x_2$  axis is toward the center, and the positive  $x_3$  axis completes a right handed system. Relative to this coordinate system, the acceleration of the spacecraft is determined by the applied thrust, a coriolis acceleration, and a centrifugal acceleration.

The case where  $\Omega = 0$  is equivalent to the problem of fuel optimal maneuvers relative to a fixed point in deep space. This problem of minimum fuel translation or its mathematical equivalent, minimum fuel rotation, has been discussed by several authors [1-5] and is a special case of other second order linear systems that have been studied [6, 7]. It is well known that the nonsingular solutions of this problem consist of intervals of full thrust and coast with at most one coast interval. Minimum fuel control of other and more general linear systems have been investigated [8 - 12] and, in general, the solutions are not so restrictive. The nonsingular fuel optimal solutions for the case where  $\Omega \neq 0$

have also been found to consist of intervals of full thrust and coast but more than one coast interval is possible [13]. We extend that result here to show that as many as three coast intervals can occur for flight times less than or equal to  $2\pi/\Omega$  and more can occur for flight times exceeding one period. We show also that there are only four boundary conditions for which singular solutions exist. Finally we present the results of computer simulation of optimal maneuvers for various boundary conditions.



## II. MATHEMATICAL ANALYSIS

The problem of minimum fuel maneuvers of a spacecraft about a body moving in a circular orbit is formulated as follows.

Let  $U$  denote the set of all Lebesgue measurable functions which map the real closed interval  $[0, t_f]$  into the closed unit ball in  $\mathbb{R}^3$ . We seek  $u \in U$  to minimize the functional

$$J[u] = \int_0^{t_f} |u(t)| dt \quad (1)$$

(where  $| \cdot |$  denotes the Euclidean norm or magnitude) subject to the differential equations

$$\begin{aligned} \dot{x}(t) &= v(t) \\ \dot{v}(t) &= Ax(t) + Bv(t) + bu(t) \end{aligned} \quad (2)$$

which hold a.e. on  $[0, t_f]$  and the boundary conditions

$$\begin{aligned} x(0) &= x_0 & x(t_f) &= x_f \\ v(0) &= v_0 & v(t_f) &= v_f \end{aligned} \quad (3)$$

where  $x_0, v_0, x_f,$  and  $v_f$  are specified points in  $\mathbb{R}^3$  and

$$A = \begin{pmatrix} 0 & 0 & 0 \\ 0 & 3\Omega^2 & 0 \\ 0 & 0 & -\Omega^2 \end{pmatrix} \quad B = \begin{pmatrix} 0 & 2\Omega & 0 \\ -2\Omega & 0 & 0 \\ 0 & 0 & 0 \end{pmatrix} \quad (4)$$

The scalar  $\Omega$  is the orbital angular speed of the body in circular orbit and the scalar  $b$  is the maximum thrust magnitude divided by the mass of the spacecraft.

Since the integrand in Eq. 1 is independent of  $x$  and  $v$  the Pontryagin Maximum Principle provides both necessary and sufficient conditions for a minimum

[14, Sec. 5.2]. For boundary conditions in which the solution is normal the Hamiltonian is

$$H = |u(t)| + p(t)^T v(t) + q(t)^T Ax(t) + q(t)^T Bv(t) + bq(t)^T u(t) \quad (5)$$

where the functions  $p$  and  $q$  which map  $[0, t_f]$  into  $\mathbb{R}^3$  are absolutely continuous solutions of the adjoint differential equations

$$\begin{aligned} \dot{p}(t) &= -A^T q(t) \\ \dot{q}(t) &= -B^T q(t) - p(t) \end{aligned} \quad (6)$$

and a nonsingular optimal control function is defined a.e. on  $[0, t_f]$  by

$$\begin{aligned} u(t) &= 0, \quad |q(t)| < 1 \\ u(t) &= -q(t)/|q(t)|, \quad |q(t)| > 1. \end{aligned} \quad (7)$$

An optimal solution in which  $|q(t)| = 1$  on a set of positive Lebesgue measure is called singular on that set.

Equation 7 shows that a nonsingular optimal control function has values that are either on the unit ball or are zero (i.e. either full thrust or coast). Moreover  $q$  determines entirely which of these situations occurs. If  $q(t)$  is outside of the unit ball a full thrust is required, whereas a coast is required if  $q(t)$  is inside the unit ball. Qualitative information about the nature of optimal solutions such as the number of thrusts and coasts or whether or not the solution is singular can be determined from the function  $q$ . We shall therefore solve Eq. 6 for  $q$  and examine the various forms that this solution can take.

Eliminating  $p(t)$  in Eq. 6 we obtain the differential equation

$$\ddot{q}(t) + B^T \dot{q}(t) - A^T q(t) = 0. \quad (8)$$

Before finding the general solution of Eq. 8 we note that  $A^T = A$  and  $B^T = -B$  so that if we eliminate  $v$  in Eq. 2 we obtain

$$\ddot{x}(t) + B^T \dot{x}(t) - A^T x(t) = bu(t). \quad (9)$$

During a coast interval in which  $u(t) = 0$  the differential equations 8 and 9 are identical. For this reason  $q(t)$  may be visualized as a point in orbit relative to a body moving in a circular orbit.

Using subscripts to denote the components of the vector  $q(t)$ , Eq. 8 may be replaced by the following system of scalar equations:

$$\begin{aligned} \ddot{q}_1(t) - 2\Omega \dot{q}_2(t) &= 0 \\ \ddot{q}_2(t) + 2\Omega \dot{q}_1(t) - 3\Omega^2 q_2(t) &= 0 \\ \ddot{q}_3(t) + \Omega^2 q_3(t) &= 0. \end{aligned} \quad (10)$$

Equation 7 shows that a boundary point  $t$  between a thrusting and coasting regime of  $u(t)$  must satisfy the condition

$$|q(t)| = 1. \quad (11)$$

The function  $|q(t)| - 1$  is called the switching function of  $u(t)$ . A value of  $t$  at which the switching function changes sign is called a switch of  $u(t)$ . Whenever a switch occurs  $u(t)$  changes from thrust to coast or from coast to thrust and conversely. Whenever a switch of  $u(t)$  occurs the solution of Eq. 10 intersects the unit sphere. Clearly the number of switches cannot exceed the number of intersection points.

The form of the solution of Eq. 10 depends on whether or not  $\Omega = 0$ . The case  $\Omega = 0$  corresponds to a problem of optimal maneuvers in deep space rather than about a circular orbit. In deep space Eq. 8 becomes

$$\ddot{q}(t) = 0 \quad (12)$$

and its general solution is

$$q(t) = -p_0 t + q_0 \quad (0 \leq t \leq t_f) \quad (13)$$

where  $p_0$  and  $q_0$  are constants in  $\mathbb{R}^3$ . Geometrically, this solution describes a straight line segment in  $\mathbb{R}^3$ . This shows, in view of Eq. 11, that an optimal maneuver in deep space can have at most two thrust intervals and one coast interval. A detailed discussion of this case which also includes singular controls can be found in [13].

There is more variety in the type of optimal maneuvers that can occur about a body in circular orbit. In the case where  $\Omega \neq 0$  the general solution of Eq. 10 is

$$\begin{aligned} q_1(t) &= 2 \rho \sin(\Omega t + \psi) - 3c_1 t + c_2 \\ q_2(t) &= \rho \cos(\Omega t + \psi) - \frac{2c_1}{\Omega} \quad (0 \leq t \leq t_f) \quad (14) \\ q_3(t) &= a \sin(\Omega t + \psi) + b \cos(\Omega t + \psi). \end{aligned}$$

Geometrically this solution resembles a helical segment if  $\rho$ ,  $c_1$ , and either  $a$  or  $b$  is nonzero. Less general situations can occur which we shall consider. Of special interest is the case in which  $a = b = 0$ . In this case the solution curve is confined to the plane of the circular orbit.

#### 1. Solution in the Orbital Plane

If the third component of each of the vectors  $x_0$ ,  $v_0$ ,  $x_f$ , and  $v_f$  in Eq. 3 is zero, then the solutions  $u(t)$ ,  $q(t)$ , and  $x(t)$  from Eqs. 7-9 are each contained in the orbital plane.

In this case the plane curve obtained from Eq. 14 resembles a type of cycloid if  $c_1$  and  $\rho$  are nonzero. The relationship to a cycloid can be demonstrated by the following transformation.

$$\gamma_1 = -q_1/2 \quad (15)$$

$$\gamma_2 = -q_2 \quad .$$

The curve defined by  $\gamma = (\gamma_1, \gamma_2)$  is a type of cycloid. If we introduce the following change of variables:

$$\begin{aligned} \theta &= \Omega t + \psi \\ \alpha &= \frac{3c_1}{2\Omega} \end{aligned} \quad (16)$$

$$c = \frac{-3c_1}{2\Omega} - \frac{c_2}{2} \quad .$$

the curve takes the standard form

$$\begin{aligned} \gamma_1 &= \alpha\theta - \rho \sin \theta + c \\ \gamma_2 &= \alpha - \rho \cos \theta + \alpha/3 \end{aligned} \quad (17)$$

This curve is a cycloid if  $\rho = |\alpha|$  and  $\rho > 0$ , a prolate cycloid if  $\rho > |\alpha| > 0$ , and a curtate cycloid if  $0 < \rho < |\alpha|$ . In each case the curve is periodic with a period of  $2\pi$ . For this reason the curve defined by  $q$  is a segment of a periodic curve having the orbital period  $2\pi/\Omega$ . It has periodic loops if and only if  $\rho > \frac{3|c_1|}{2\Omega} > 0$ .

The nature of the optimal thrusting sequence is determined by the relationship of  $q(t)$  to the unit circle in the orbital plane. This is depicted in Fig. 1 for the case where  $\Omega = 0$ . Since a straight line can intersect a circle in at most two points, it is seen that a fuel optimal maneuver in deep space can have at most two switches. If  $\Omega \neq 0$  more switches can occur as is demonstrated in Fig. 2 where  $q(t)$  takes a cycloidal shape. There is an essential difference between the deep space case and the circular orbit case even if  $t_f$  is small. This is because even

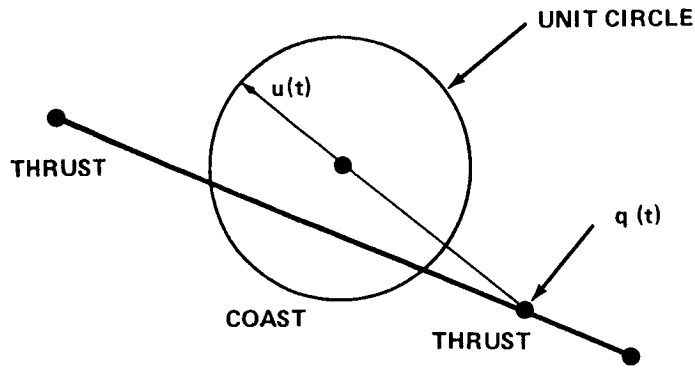


FIGURE 1. NATURE OF FUEL OPTIMAL THRUSTING SEQUENCE IN DEEP SPACE

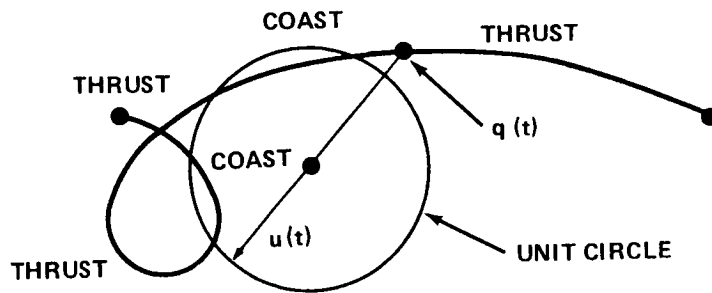


FIGURE 2. NATURE OF FUEL OPTIMAL THRUSTING SEQUENCE ABOUT A POINT MOVING IN CIRCULAR ORBIT

though  $\theta$  may be restricted to an arbitrarily small interval, there are values of the constants  $\alpha$ ,  $\rho$ , and  $c$  so that a prolate cycloid can have a complete loop on that interval. For this reason even if  $t_f$  is small there are values of  $\rho$ ,  $c_1$ , and  $c_2$  so that  $q(t)$  can intersect the unit circle more than twice.

Equation 15 transforms the unit circle into the ellipse

$$\gamma_1^2 + 4\gamma_2^2 = 4. \quad (18)$$

This ellipse can intersect the curve defined by Eq. 17 at most six times in one period and more than six times over larger intervals than a period. This indicates that at most six switches are possible during one period of a fuel optimal maneuver about a body in circular orbit and more are possible for longer flight times.

A case where six switches occur is presented in Fig. 3 where the curve  $q(t)$  intersects the unit circle at six points. This corresponds to a "thrust-coast-thrust-coast-thrust-coast-thrust" maneuver, a thrusting sequence consisting of seven phases. This information can be seen more easily from Fig. 4 which presents the magnitude of  $q$  vs the orbital angle  $\theta$  which is defined in Eq. 16. The thrust intervals occur where  $|q|$  is greater than one and the coast intervals occur where  $|q|$  is less than one. A seven phase maneuver can also occur for any smaller flight time if  $\rho$ ,  $c_1$ , and  $c_2$  are picked correctly but these maneuvers for small flight times may require that some of the boundary conditions defined by Eq. 3 have enormous magnitude.

We now consider the degenerate cases.

If  $c_1 = 0$  and  $\rho \neq 0$  then  $q(t)$  defines a segment of an ellipse whose ratio of major-to-minor axis is two. An ellipse can intersect the unit circle in at most four points so the maximum number of switches that can occur in an optimal maneuver in this case is four in one period although more can occur for flight times exceeding one period.

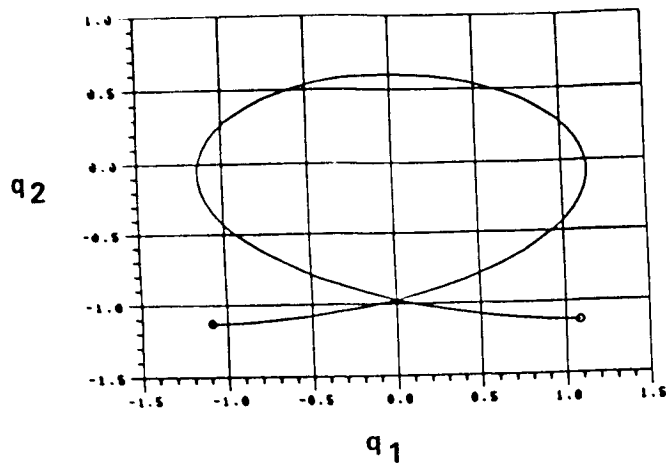


FIGURE 3 : A SEVEN PHASE OPTIMAL THRUSTING SEQUENCE IN ONE PERIOD

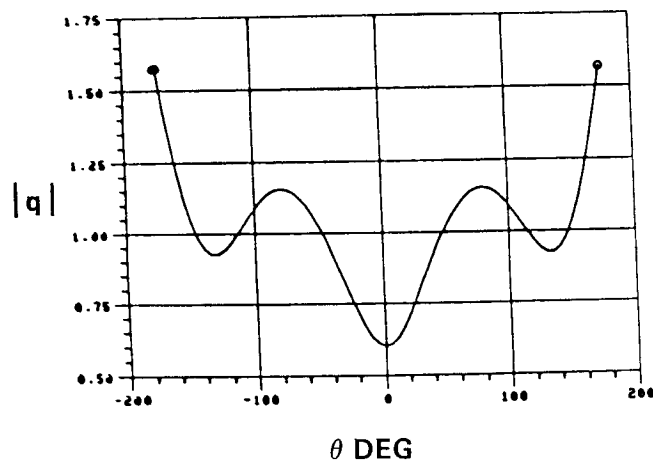


FIGURE 4 : THE ABSOLUTE VALUE OF  $q$  OVER ONE PERIOD FOR THE SEVEN PHASE OPTIMAL THRUSTING SEQUENCE



If  $\rho = 0$  and  $c_1 \neq 0$  then  $q(t)$  defines a straight line segment as in the deep space situation and at most two switches are possible.

If both  $c_1$  and  $\rho$  are zero, no switches can occur. This is the only situation in the orbital plane case where singular solutions can occur and this happens if  $c_2 = \pm 1$ . This fact will be shown in the material which follows.

## 2. Solutions Out of the Orbital Plane

We now examine the other cases where  $q(t)$  as defined by Eq. 14 is not in the orbital plane.

We first consider the cases where  $c_1 \neq 0$ .

We note, first of all, that singular solutions are impossible for these cases because  $c_1 \neq 0$  in Eq. 14 shows that Eq. 11 cannot be satisfied identically.

If  $a$  and  $b$  are not both zero and if  $\rho$  is nonzero then the solution of Eq. 14 defines a helical type path that intersects the unit sphere on at most six points during one period. This establishes at most six switches of  $u(t)$  during one period of an optimal maneuver.

If  $\rho = 0$  and  $a$  and  $b$  are not both zero then Eq. 14 defines a shifted sine curve. This curve can intersect the unit sphere at six points but not more. In this situation also an optimal maneuver has at most six switches in one period.

We now consider the cases in which  $c_1 = 0$ .

Singular solutions occur if and only if Eq. 11 is satisfied identically, that is

$$b^2 - a^2 = 3\rho^2, ab = 0, c_2\rho = 0, \rho^2 + b^2 + c_2^2 = 1. \quad (19)$$

Equation 19 is satisfied only in the following cases:

$$\rho = 1/2, c_2 = 0, a = 0, b = \pm\sqrt{3}/2 \quad (20)$$

$$\rho = 0, c_2 = \pm 1, a = 0, b = 0. \quad (21)$$

These are the only cases where singular solutions occur. Equation 20 provides the only cases in which singular solutions exist outside of the orbital plane and Eq. 21 establishes the existence of the singular solutions in the orbital plane previously mentioned.

In the case where  $\rho \neq 0$ , Eq. 14 defines, in general, an ellipse which either intersects the unit sphere in at most four points or which is identically on the unit sphere. The latter is the singular situation described by Eq. 20. The former indicates that at most four switches in one period are possible for a nonsingular optimal maneuver in this case.

If  $\rho = 0$  and  $a$  and  $b$  are not both zero then Eq. 14 defines a point moving with simple harmonic motion along a line segment. This moving point crosses the unit sphere at no more than four values of  $t$ . In this case also no more than four switches can occur during one period of an optimal maneuver.

### III. COMPUTER SIMULATIONS

This section presents the flight path and switching function for several fuel optimal maneuvers in a plane, both in deep space and about a body in circular orbit. These results were obtained by solution of a two point boundary value problem using a program written by Roger R. Burrows of the Flight Mechanics Branch of the George C. Marshall Space Flight Center.

Figures 5-10 are presented to illustrate optimal maneuvers in deep space for a variety of boundary conditions. Since only the basic shapes are of interest here Eq. 2 is normalized with  $b = 1$  and the flight time  $t_f$  is four. Intervals of thrust or coast can be determined from the regions where the switching function depicted on the left is respectively positive or negative.

Figures 11-12 compare an optimal soft rendezvous with a body fixed in deep space and an optimal soft rendezvous with a body in circular orbit for identical initial conditions. These simulations were based on a spacecraft mass of approximately 3400 kilograms, maximum thrust of 267 Newtons, and a flight time of 600 seconds. The upper part of the figures illustrates the optimal switching function and flight path shape for the deep space rendezvous ( $\Omega = 0$  rad/sec) whereas the lower part presents this information for rendezvous with a body moving in a 435 kilometer altitude circular orbit ( $\Omega = .001122$  rad/sec). The similarities and differences in shape are apparent.

Figure 13 presents an optimal soft rendezvous of a spacecraft in the 435 kilometer altitude circular orbit with a body one kilometer behind in the same orbit for flight times of 600 seconds, one half period (2800 sec), and three fourths period (4200 sec). The mass and maximum thrust are the same as in the previous case.

Figure 14 also presents a soft rendezvous in which the same spacecraft is ferrying a mass nine times heavier than itself to a body in the 435 kilometer circular orbit. The spacecraft begins one kilometer above the body with the same velocity. The flight time is long, six sevenths of a period (4800 sec) and the optimal thrusting function has four switches. The thrusting sequence is "thrust-coast-thrust-coast-thrust."

Figure 15 depicts a situation in which the spacecraft pushes a mass nine times heavier than itself out of circular orbit to a point in an elliptical orbit 73 kilometers behind. This optimal maneuver has a flight time of one period (5600 sec) and the optimal switching function is determined from the curve  $q(t)$  presented in Fig. 3. This can be seen from the similarity between Fig. 4 and the switching function shown in Fig. 15. This is an example of an optimal maneuver which has a thrusting sequence requiring the maximum of seven phases in one period.

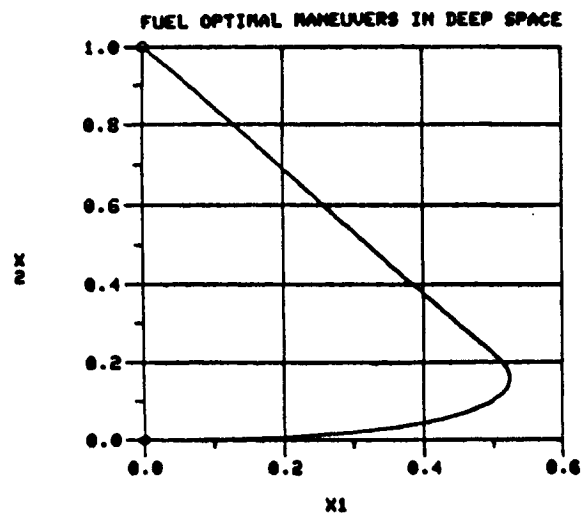
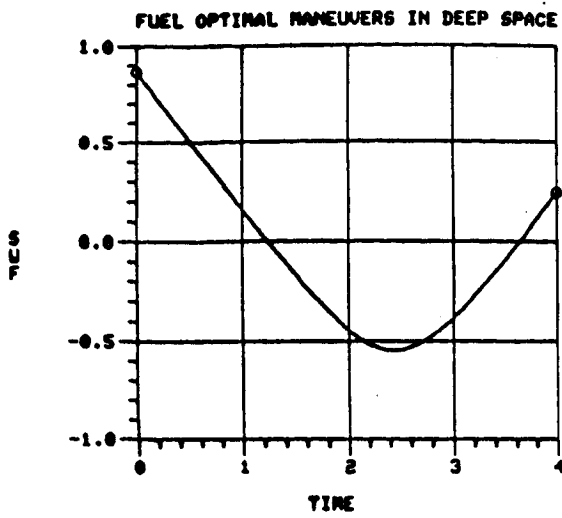


FIGURE 5 : SWITCHING FUNCTION AND FLIGHT PATH FOR  $X(0) = (0, 0)$ ,  
 $V(0) = (1, 0)$ ,  $X(TF) = (0, 1)$ ,  $V(TF) = (0, 0)$

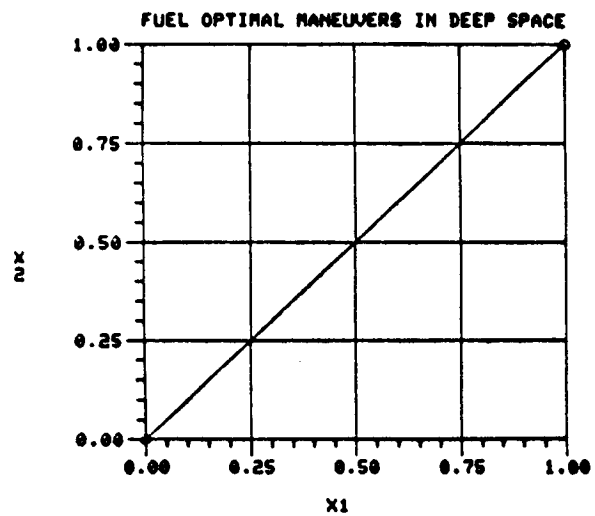
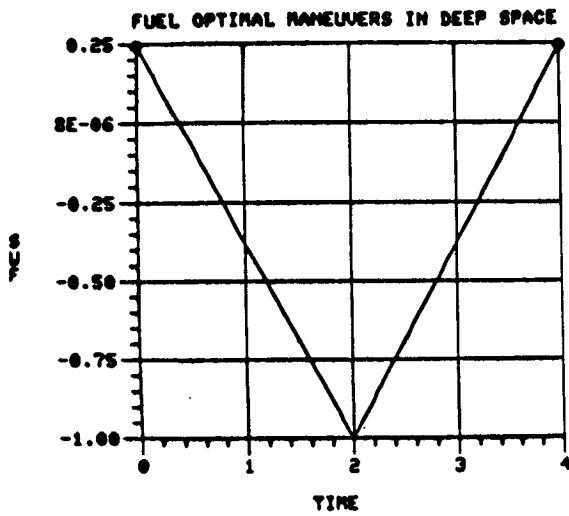


FIGURE 6 : SWITCHING FUNCTION AND FLIGHT PATH FOR  $X(0) = (0, 0)$ ,  
 $V(0) = (0, 0)$ ,  $X(TF) = (1, 1)$ ,  $V(TF) = (0, 0)$

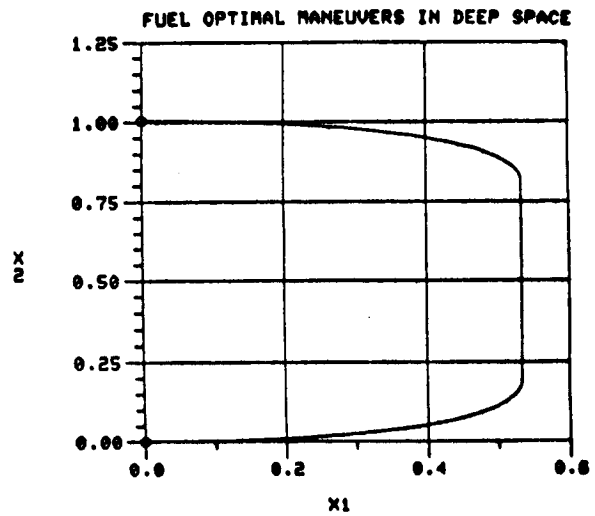
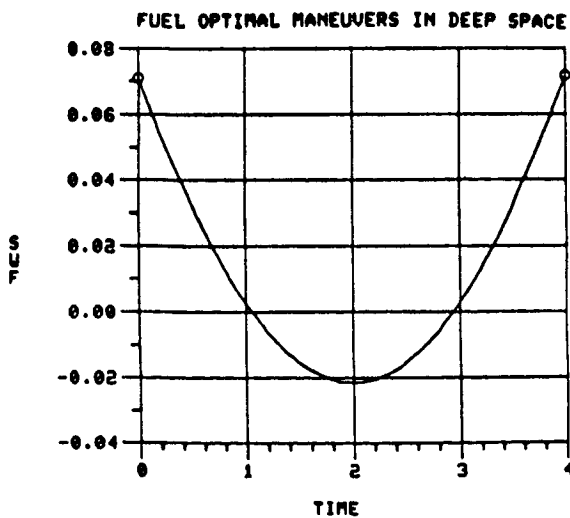


FIGURE 7 : SWITCHING FUNCTION AND FLIGHT PATH FOR  $X(0) = (0, 0)$   
 $V(0) = (1, 0)$ ,  $X(TF) = (0, 1)$ ,  $V(TF) = (-1, 0)$

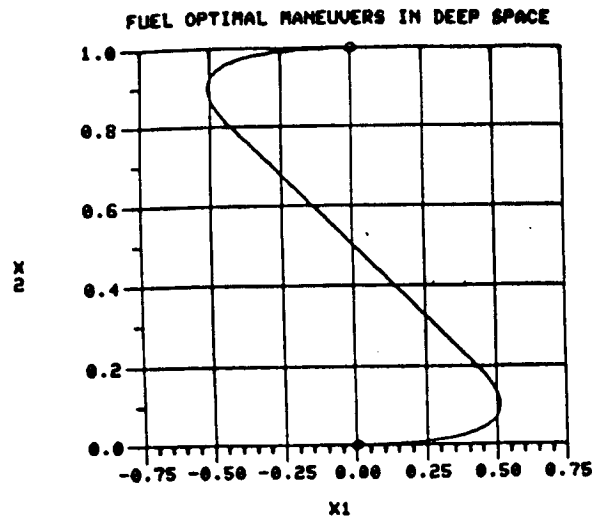
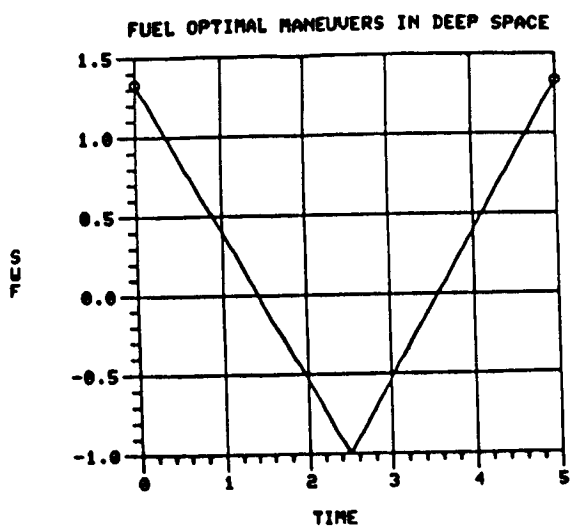


FIGURE 8 : SWITCHING FUNCTION AND FLIGHT PATH FOR  $X(0) = (0, 0)$ ,  
 $V(0) = (1, 0)$ ,  $X(TF) = (0, 1)$ ,  $V(TF) = (1, 0)$

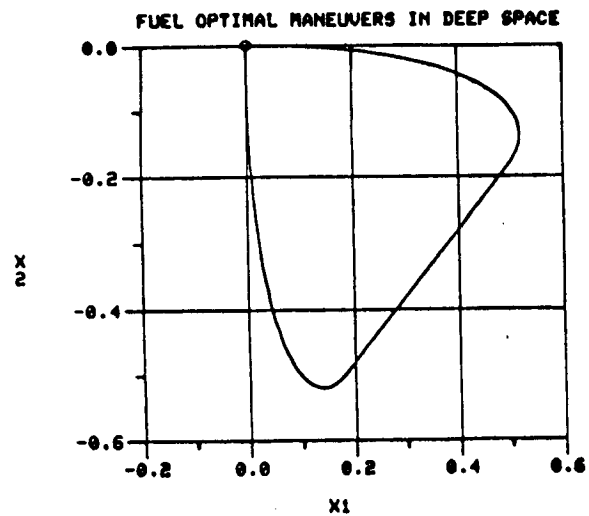
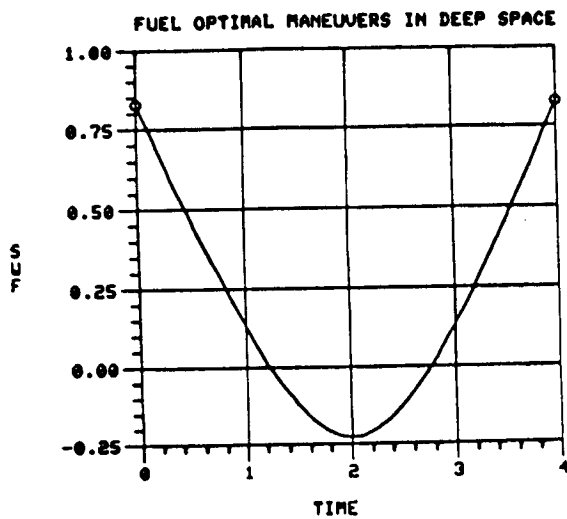


FIGURE 9 : SWITCHING FUNCTION AND FLIGHT PATH FOR  $X(0) = (0, 0)$ ,  
 $V(0) = (1, 0)$ ,  $X(TF) = (0, 0)$ ,  $V(TF) = (0, 1)$

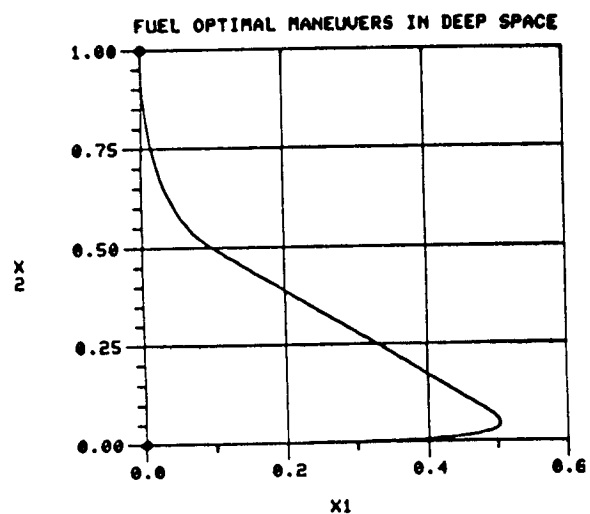
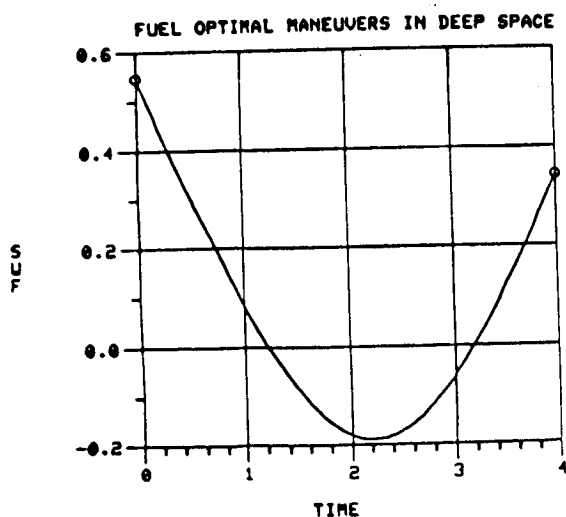
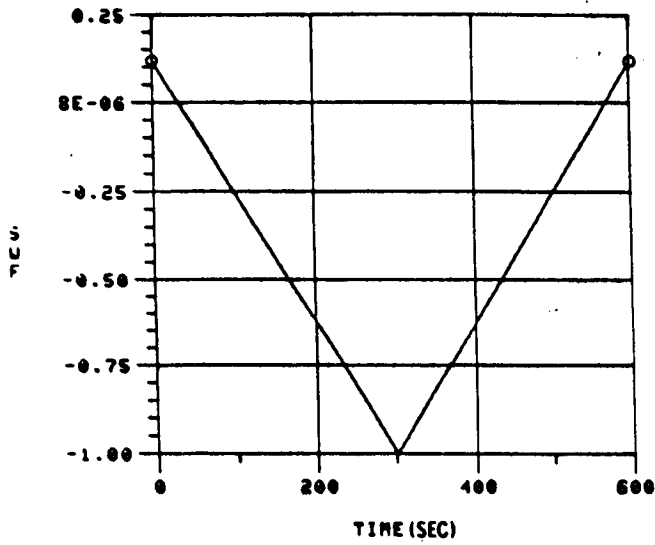
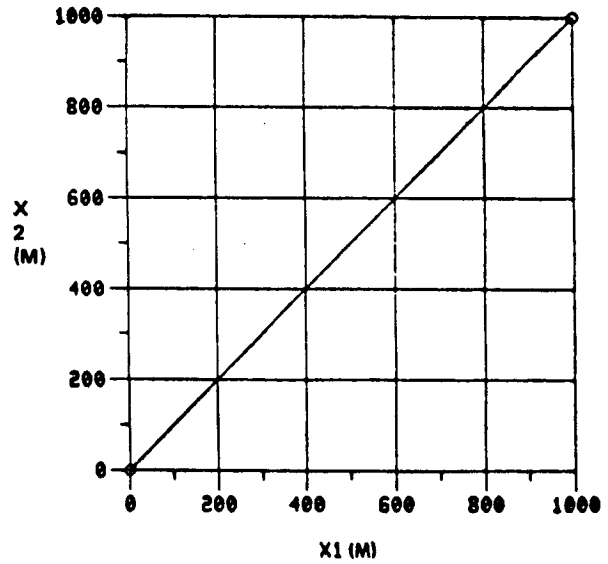


FIGURE 10 : SWITCHING FUNCTION AND FLIGHT PATH FOR  $X(0) = (0, 0)$ ,  
 $V(0) = (1, 0)$ ,  $X(TF) = (0, 1)$ ,  $V(TF) = (0, 1)$

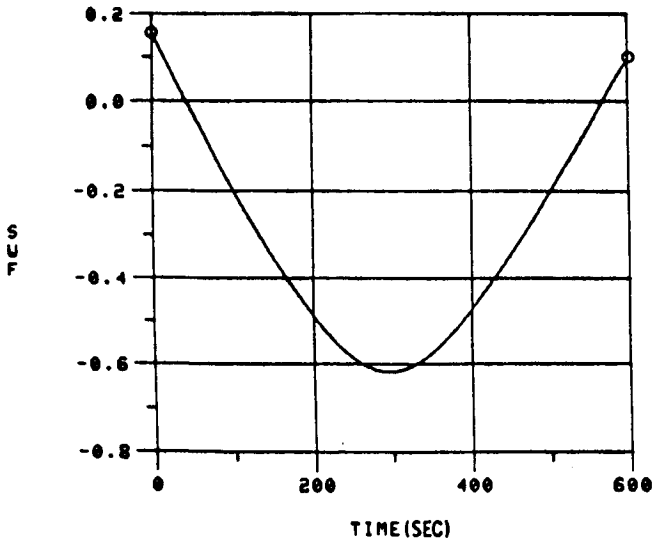
FUEL OPTIMAL MANEUVERS IN DEEP SPACE



FUEL OPTIMAL MANEUVERS IN DEEP SPACE



FUEL OPTIMAL MANEUVERS ABOUT A CIRCULAR ORBIT



FUEL OPTIMAL MANEUVERS ABOUT A CIRCULAR ORBIT

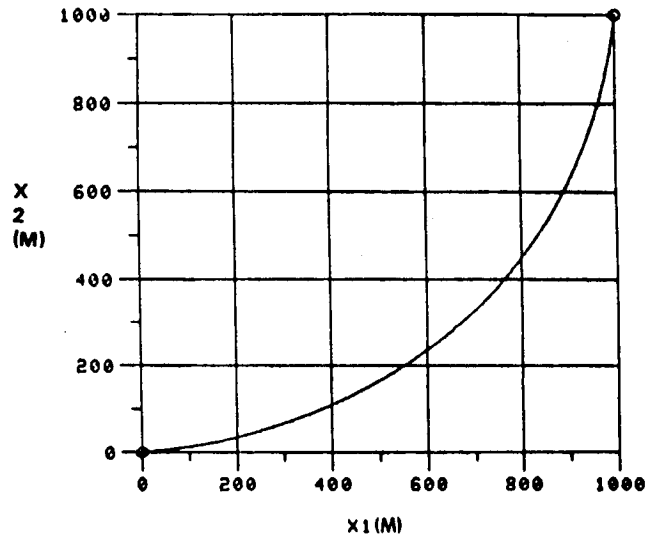
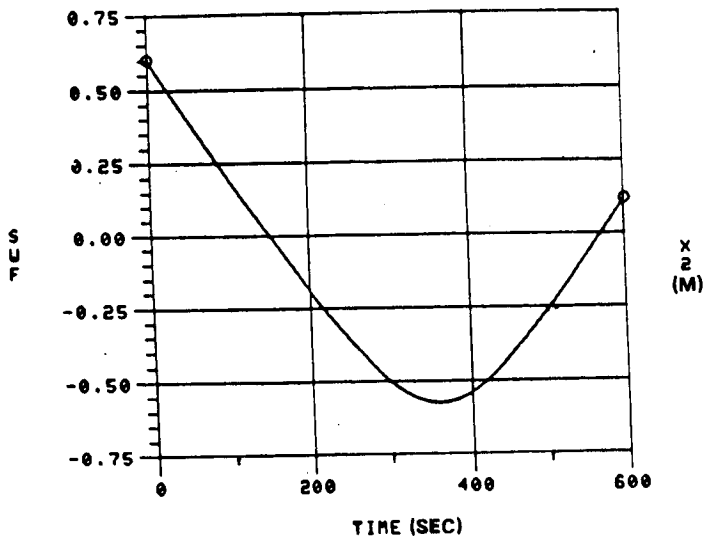
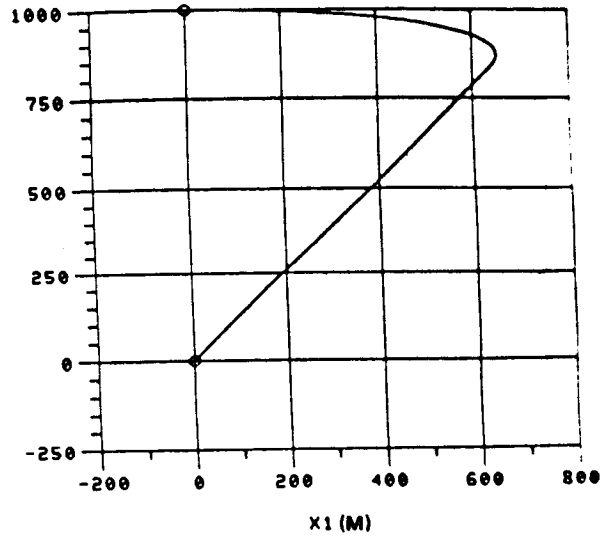


FIGURE 11 : COMPARISON OF SWITCHING FUNCTIONS AND FLIGHT PATHS FOR DEEP SPACE AND 435 KM. ALTITUDE CIRCULAR ORBIT:  
 $X(0) = (1000, 1000)$ ,  $V(0) = (0, 0)$ ,  $X(TF) = (0, 0)$ ,  $V(TF) = (0, 0)$

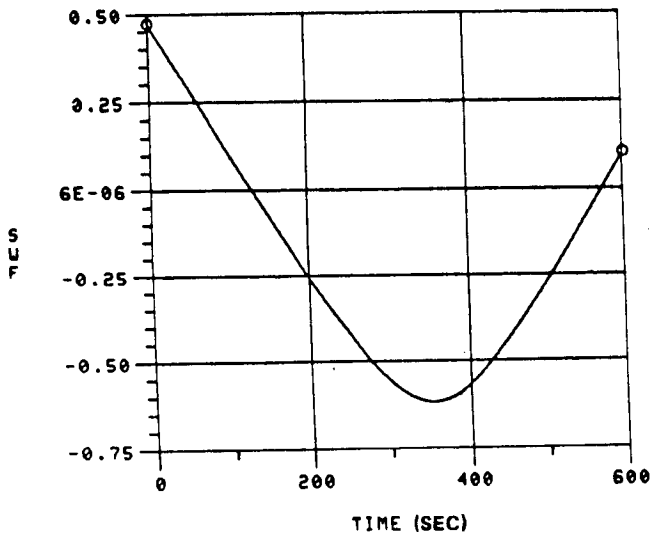
FUEL OPTIMAL MANEUVERS IN DEEP SPACE



FUEL OPTIMAL MANEUVERS IN DEEP SPACE



FUEL OPTIMAL MANEUVERS ABOUT A CIRCULAR ORBIT



FUEL OPTIMAL MANEUVERS ABOUT A CIRCULAR ORBIT

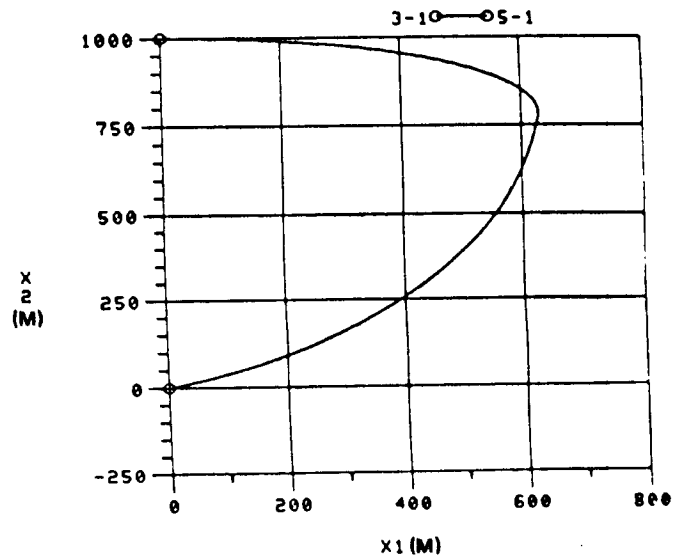
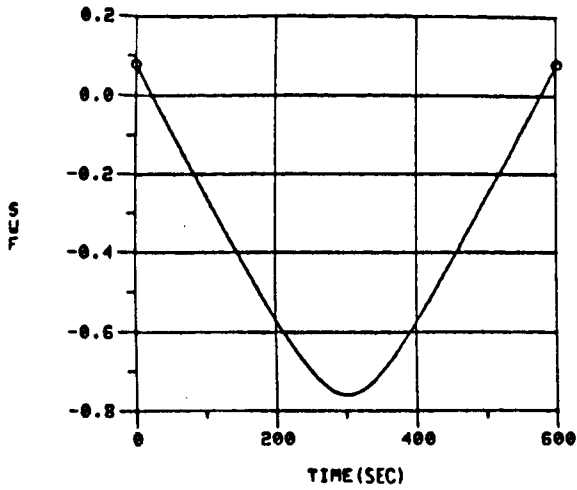


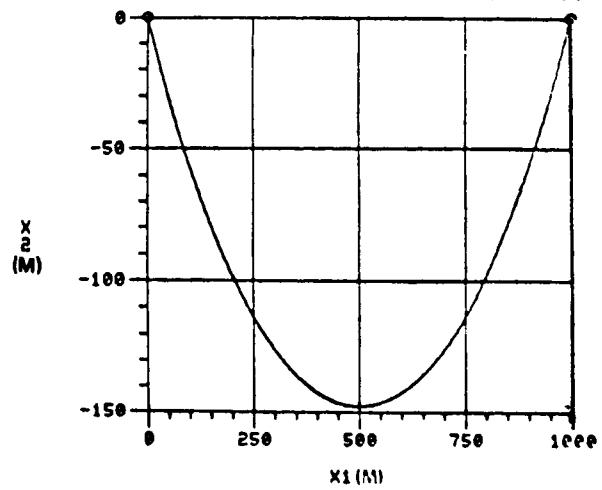
FIGURE 12 : COMPARISON OF SWITCHING FUNCTIONS AND FLIGHT PATHS FOR DEEP SPACE AND 435 KM. ALTITUDE CIRCULAR ORBIT:  
 $X(0) = (0, 1000)$ ,  $V(0) = (10, 0)$ ,  $X(TF) = (0, 0)$ ,  $V(TF) = (0, 0)$



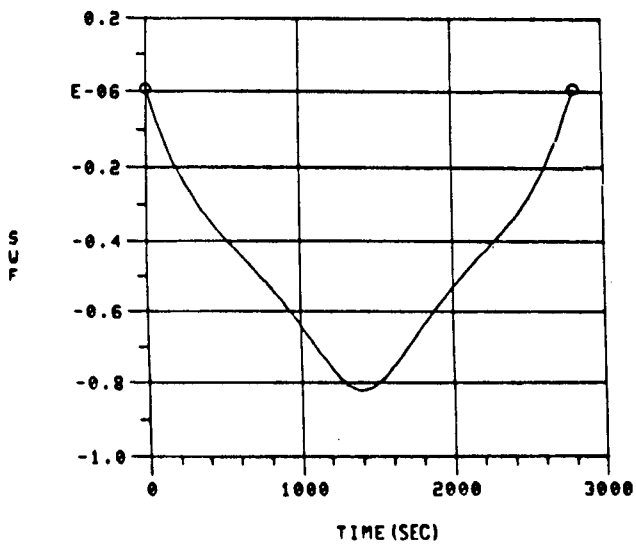
FUEL OPTIMAL MANUEVERS ABOUT A CIRCULAR ORBIT



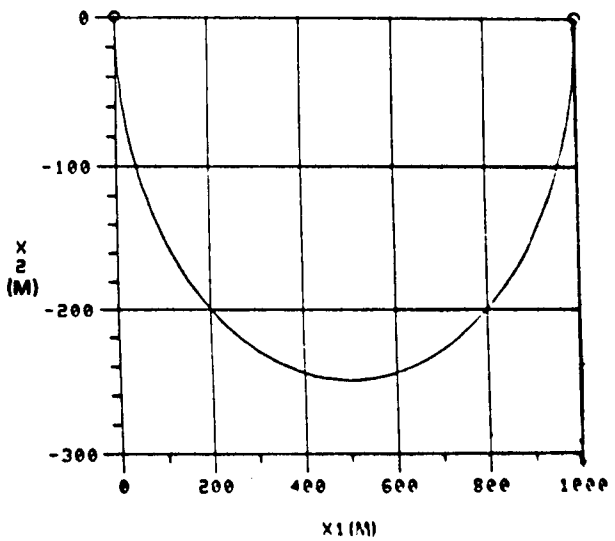
FUEL OPTIMAL MANUEVERS ABOUT A CIRCULAR ORBIT



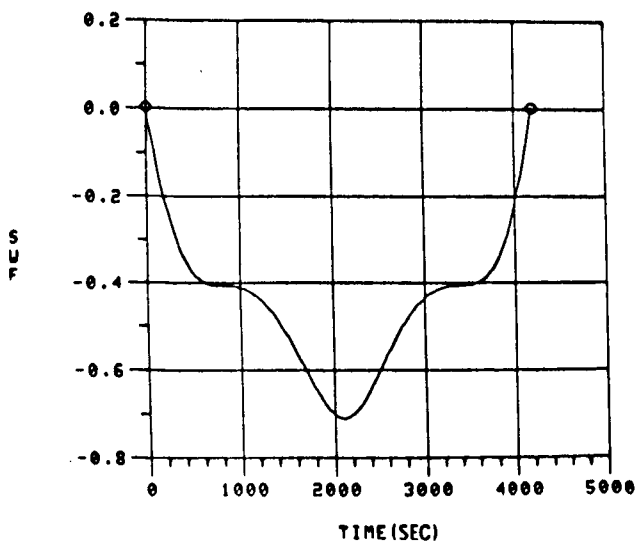
FUEL OPTIMAL MANUEVERS ABOUT A CIRCULAR ORBIT



FUEL OPTIMAL MANUEVERS ABOUT A CIRCULAR ORBIT



FUEL OPTIMAL MANUEVERS ABOUT A CIRCULAR ORBIT



FUEL OPTIMAL MANUEVERS ABOUT A CIRCULAR ORBIT

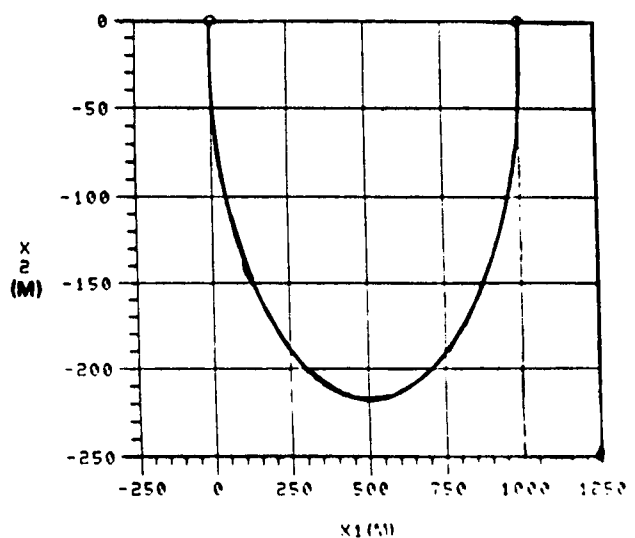
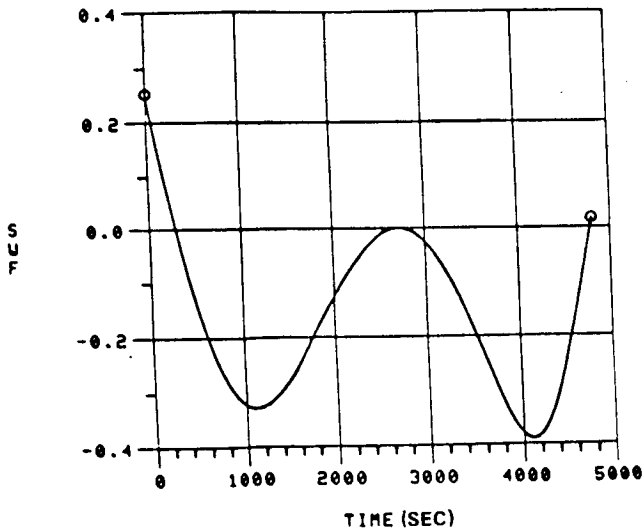


FIGURE 13 : SWITCHING FUNCTION AND FLIGHT PATH FOR DIFFERENT FLIGHT TIMES FOR 435 KM. CIRCULAR ORBIT:  $x(0) = (1000, 0)$ ,  $v(0) = (0, 0)$ ,  $x(TF) = (0, 0)$ ,  $v(TF) = (0, 0)$

FUEL OPTIMAL MANEUVERS ABOUT A CIRCULAR ORBIT



FUEL OPTIMAL MANEUVERS ABOUT A CIRCULAR ORBIT

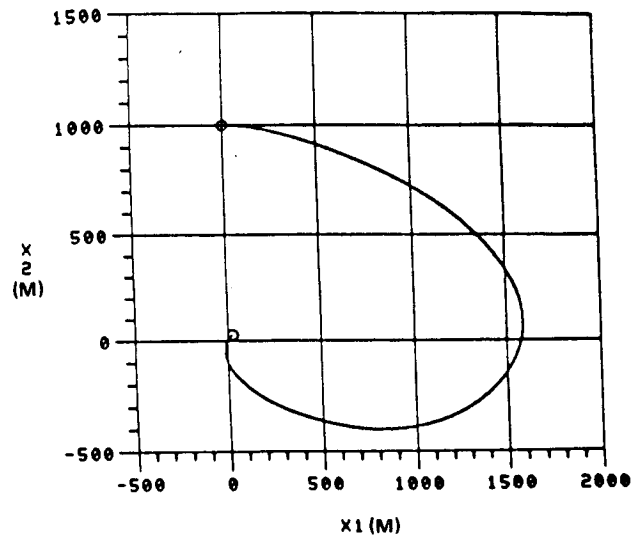
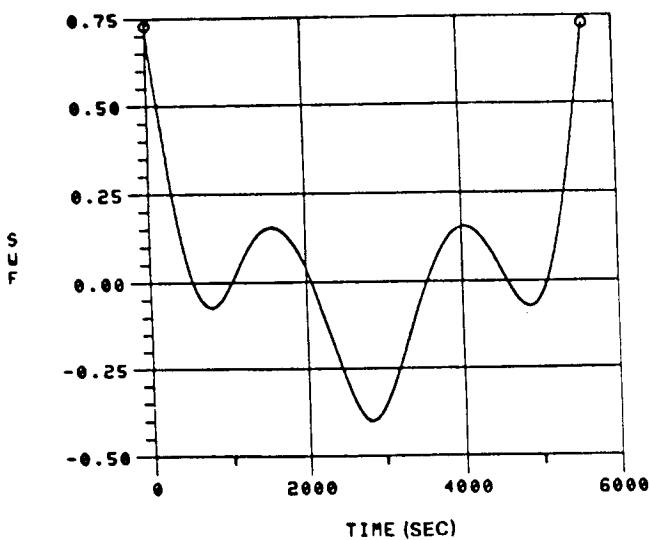


FIGURE 14 : INSERTION OF MASS FROM ELLIPTICAL INTO 435 KM. CIRCULAR ORBIT:  $X(0) = (0, 1000)$ ,  $V(0) = (0, 0)$ ,  $X(TF) = (0, 0)$ ,  $V(TF) = (0, 0)$ , OPTIMAL MANEUVER REQUIRES MID-COURSE THRUST

FUEL OPTIMAL MANEUVERS ABOUT A CIRCULAR ORBIT



FUEL OPTIMAL MANEUVERS ABOUT A CIRCULAR ORBIT

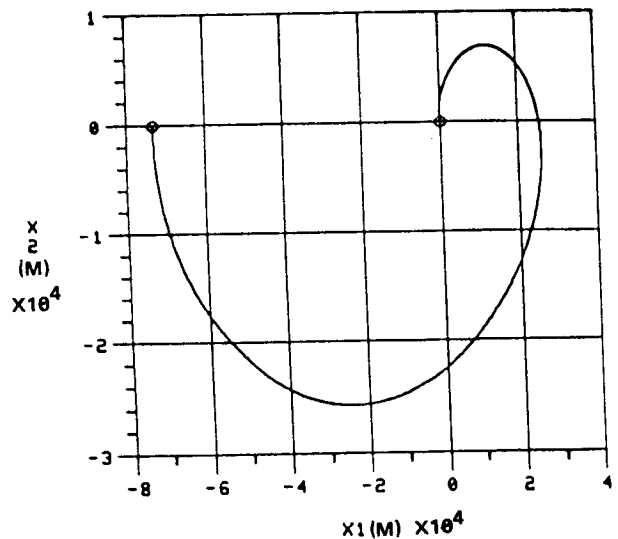


FIGURE 15 : AN OPTIMAL MANEUVER WITH FOUR THRUSTS AND THREE COASTS IN ONE PERIOD (5600 SEC):  $X(0) = (0, 0)$ ,  $V(0) = (0, 0)$ ,  $X(TF) = (-73000, 0)$ ,  $V(TF) = (0, 35)$

#### IV. CONCLUSIONS

Several different forms of solutions to Eq. 10 can occur. If  $\Omega = 0$  the solution is a line segment and the optimal control consists of intervals of full thrust and coast with at most two switches. If  $\Omega \neq 0$  the solution may be a helical type segment, a shifted sine curve segment, a horizontal straight line segment, a prolate or curtate cycloidal type segment, or a segment of an ellipse. The optimal control consists of intervals of full thrust and coast in each of these cases. More than two switches are possible even for small flight times. If  $c_1 \neq 0$  there is a maximum of six switches possible in one period. If  $c_1 = 0$  the maximum number of switches that can occur in one period is four.

If  $\Omega \neq 0$  only two cases exist in which singular solutions (defined by Eq. 20) can occur outside of the orbital plane. Also only two cases where singular solutions (defined by Eq. 21) exist can occur on the orbital plane.

Computer simulations were run for solution of Eqs. 2, 3, 6, and 7 for cases where  $\Omega = 0$  and where  $\Omega = 2\pi/5600$  rad/sec. It was found generally that for small flight times and boundary conditions of small magnitudes the optimal maneuvers contained no more than two switches. Boundary value problems whose solutions consisted of four switches and six switches were found.

## REFERENCES

1. I. Flugge-Lotz and H. Marbach, "The Optimal Control of Some Attitude Control Systems for Different Performance Criteria," Trans. ASME J. Appl. Mech. (1964) pp. 107-115.
2. J. S. Meditch, "On Minimal Fuel Satellite Attitude Controls," Preprints of the 1963 JACC.
3. L. Schwartz, "Minimum Energy Attitude Control for a Class of Electric Propulsion Devices," Proceedings, 1964 JACC.
4. D. A. Conrad, "Minimum Fuel Closed-Loop Translation," AIAA J. (May 1965).
5. W. F. Keller, "Study of Spacecraft Hover and Translation Modes Above the Lunar Surface," AIAA Preprint 64-341.
6. H. O. Ladd and R. Friedland, "Minimum Fuel Control of a Second Order Linear Process With a Constraint on Time-to-Run," Trans. ASME J. Appl. Mech. (1964) pp. 165-176.
7. D. R. Snow, "Singular Optimal Controls For a Class of Minimum Effort Problems," SIAM J. Control, (1964) pp. 203-219.
8. M. Athans, "Minimum-Fuel Control of Second-Order Systems With Real Poles," 1963 JACC, pp. 232-240.
9. A. J. Craig and I. Flugge-Lotz, "Investigation of Optimal Control With Minimum-Fuel Consumption Criteria for a Fourth-Order Plant With Two Control Inputs: Synthesis of an Efficient Sub-Optimal Control," 1963 JACC.
10. M. Athans, "On Optimal Control of Self Adjoint Systems," 1963 JACC.
11. W. C. Grimmell, "The Existence of Piecewise Continuous Fuel Optimal Controls," SIAM J. Control (1967), pp. 515-519.
12. D. L. Grey and M. Athans, "Computation of Fuel-Optimal Control via Newton's Method - Theory," 1968 JACC.
13. T. E. Carter, "Fuel Optimal Maneuvers for Spacecraft with Fixed Thrusters," NASA CR -161855 (1981).
14. E. B. Lee and L. Markus, Foundations of Optimal Control Theory, Wiley, 1967.